Scientific Research Publishing

Advances in Aerospace Science and Technology, 2024, 9, 167-177
https://www.scirp.org/journal/aast
ISSN Online: 2473-6724
ISSN Print: 2473-6708

Dynamic Characterization of Helicopter Main Reducer Planetary Drive System under Several Typical Flight Conditions

Lin Yang*, Fengqiang Qian, Xiangyan Meng, Wenjin Zhou

Hunan Provincial Key Laboratory of Health Maintenance for Mechanical Equipment, Hunan University of Science and Technology, Xiangtan, China
Email: *yl_152114@163.com

How to cite this paper: Yang, L., Qian, F.Q., Meng, X.Y.and Zhou, W.J. (2024) Dynamic Characterization of Helicopter Main Reducer Planetary Drive System under Several Typical Flight Conditions. *Advances in Aerospace Science and Technology*, **9**, 167-177.
https://doi.org/10.4236/aast.2024.94013

Received: November 25, 2024
Accepted: December 20, 2024
Published: December 23, 2024

Abstract

The transmission system is a critical power component of helicopters, playing an indispensable role in power transmission. Among its key elements, the planetary gear system is an essential part of the helicopter transmission architecture. Establishing a dynamic model of the helicopter transmission system and analyzing the dynamic response of the planetary gear system under varying flight conditions are crucial for enhancing the system's performance and safety. In this study, the transmission system is modeled comprehensively using the lumped mass method and the finite element method, and the dynamic characteristics of the planetary gear system, as reflected on the main gearbox casing under different flight scenarios, are examined. The findings reveal that the resonance frequencies of the planetary gear system remain consistent across various flight conditions, indicating that these frequencies are governed by the inherent structural and dynamic properties of the system. However, the vibration amplitudes at resonance points differ depending on the flight condition. Specifically, the resonance amplitudes at 0.057 kHz and 0.093 kHz during Hovering are significantly lower than those in other conditions, demonstrating that operational scenarios directly influence vibration response.

Keywords

Helicopter, Transmission System, Dynamic Modeling, Planetary Drive System, Flight Condition

1. Introduction

Helicopters are vital aerospace vehicles with unparalleled advantages over other aircraft, finding extensive applications in disaster relief, emergency rescue, tourism, counter-terrorism, and national security. Their role is indispensable in economic development and defense. The transmission system, a critical and non-redundant core component of helicopters, typically comprises the main gearbox, intermediate gearbox, tail gearbox, main drive shaft, and tail drive shaft [1]. This system serves as the link between the engine and the rotors, transmitting torque and power at specified gear ratios to the main rotor, tail rotor, and auxiliary components. As the primary mechanism for power transfer, its performance directly influences the flight characteristics and safety of the helicopter.

The helicopter's transmission system operates under complex dynamics due to the numerous rotating components, rich vibration sources, and the interaction of the rotor and tail rotor with turbulent flow fields. Consequently, the transmission system's performance is a critical determinant of helicopter functionality. In recent years, advancements in aviation technology have increased the emphasis on dynamic modeling and response analysis of helicopter transmission systems.

For instance, Bao and Yun [2] designed a two-stage variable-speed transmission system, developed a dynamic model considering multiple factors, and analyzed its inherent properties and dynamic response through numerical simulations. Their findings indicated that increasing input power and reducing input speed improved system dynamics. Wei and Chen [3] established a helicopter-engine coupling model validated using UH-60A helicopter data, demonstrating that engine load variations could cause rotor speed fluctuations, affecting maneuverability. Chen *et al.* [4] constructed a prediction model for the dynamic response of the tail transmission system based on rigid-flexible coupling multi-body dynamics, which was validated through experimental simulations. The model accurately predicted vibration acceleration errors within a range of −23.9% to 20.6% under variable speed and load conditions, providing theoretical and experimental foundations for high-reliability helicopter operations. Ni *et al.* [5] addressed torsional vibration in the rotor shaft system of a coaxial helicopter transmission system. Adjusting shaft diameters or excitation frequencies effectively reduced torsional resonance, guiding rotor shaft design improvements. Li *et al.* [6] proposed a configuration for a variable-speed helicopter transmission system, achieving stable speed transitions and continuous power delivery across different flight modes. Long *et al.* [7] studied the coupled vibration characteristics of the drive shaft and casing system using finite element methods and experimental tests, offering valuable insights for dynamic design. Zeng *et al.* [8] developed an innovative transmission system design methodology based on graph theory and state-space models. Luo *et al.* [9] introduced a case-based design method for helicopter main gearboxes, optimizing gear ratio distributions to minimize system weight. Lastly, Zhu *et al.* [10] investigated the dynamic behavior of helical bevel gear systems in intermediate and tail gearboxes, constructing a coupled dynamic model and analyzing the impact of key parameters on system vibration, providing theoretical support for tail transmission design.

In summary, recent research has significantly advanced the dynamic modeling and response analysis of helicopter transmission systems. However, most studies focus on individual components rather than the coupled dynamics of the entire system. Therefore, using the lumped mass method and the finite element method to develop a holistic coupled model for the helicopter transmission system and analyzing the dynamic behavior of planetary gear systems under typical flight conditions is of paramount importance.

2. Dynamic Modeling of Transmission System

The present study delineates the gear transmission system, which is predominantly constituted of conical gears, cylindrical spur gears, and associated drive shafts. The overall dynamic model of the helicopter transmission system was successfully established by using the concentrated mass method and the finite element method and combining the relevant system parameters. Among them, some shaped parts such as gear shaft, magazine and coupling parts are modeled by the finite element method, while gears and bearings are modeled dynamically by the concentrated mass method. The subsequent discussion will concentrate on elucidating the intricacies of the drive shaft subsystem and the planetary gear mechanism, which are integral components of the overall system.

2.1. Dynamic Modeling of Helicopter Shaft System

As a torque transmission and support mechanism, the structural characteristics of the shaft system significantly influence the dynamic performance of the transmission system. In engineering practice, shaft systems are often modeled dynamically alongside gear systems, as they function as both support and torque transmission components. To enhance modeling and computational efficiency, the shaft system and gear pairs are typically discretized into multiple elements for equivalent calculation. Using the lumped parameter method, dynamic modeling considers six degrees of freedom for each shaft segment. The equivalence principle ensures that the kinetic energy and elastic deformation energy remain consistent before and after the transformation.

In this approach, rotating components at the input end of the horizontal transmission shaft in the helicopter's main gearbox is equivalent to disk 1, while those of the intermediate gearbox are represented as disks $i-4$ and $i-3$, and the tail gearbox as disks $i-2$ and $i-1$. The tail rotor is simplified as disk i. The intermediate components of the gearboxes are connected by meshing stiffness, and elements such as couplings on the shaft bearings that rotate with the shaft are modeled as disks 2 and 3, linked via the torsional stiffness of the shaft. This transforms the tail transmission system of the helicopter into a series-connected system of shaft segments and disks.

Each disk is treated as a rotational disk at a support point, transmitting torque and rotational motion through the shaft segments. Consequently, the tail transmission system forms a multi-support drive shaft system, where varying rotational speeds occur due to the intermediate gearbox and differences between horizontal and tail bevel shafts. For analytical convenience, all components are equivalently reduced to the engine output shaft, with the horizontal transmission shaft serving as the equivalent component. This equivalence involves substituting each segment's inertia, elasticity, torque, and angular displacement with equivalent quantities on the simplified component. As depicted in Figure 1, the torsional dynamics model of a transmission system incorporating gears and shafts is presented.

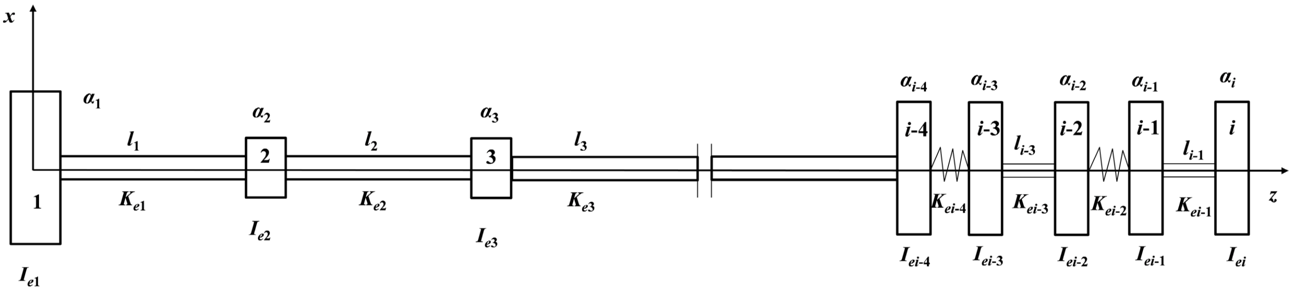

Figure 1. The torsional dynamics model of a transmission system incorporating gears and shafts.

Upon discretizing the transmission system into n discrete elements, the dynamic model of the system is characterized by n degrees of freedom. α is the torsional angular displacement of each equivalent disk. The corresponding generalized coordinates are detailed hereinafter:

$$\alpha = \left\{\alpha_1, \alpha_2, \cdots, \alpha_k, \alpha_{k+1}, \cdots, \alpha_i, \alpha_{i+1}, \cdots, \alpha_{n-1}, \alpha_n\right\} \tag{1}$$

The generalized dynamic equations of the transmission system are:

$$I\ddot{\theta} + C\dot{\theta} + K\theta = P \tag{2}$$

where I is the moment of inertia matrix:

$$I = diag\left[I_1 \quad I_2 \quad I_3 \quad I_4 \quad \cdots \quad I_{n-2} \quad I_{n-1} \quad I_n\right]^{\mathrm{T}} \tag{3}$$

J represents the rotational inertia of the equivalent disks; C denotes the torsional damping matrix, K signifies the torsional stiffness matrix, and P indicates the applied torque matrix, with their respective expressions detailed subsequently:

$$C = \begin{bmatrix}
k_1 & -k_1 & & & & & & & \\
-k_1 & k_1 + k_2 & -k_2 & & & & & & \\
 & -k_2 & k_2 + k_3 & \ddots & & & & & \\
 & & & \ddots & & & & & \\
 & & & \ddots & K_1 r_1^2 + k_{n-5} & -K_1 r_1 r_2 & & & \\
 & & & & -K_1 r_1 r_2 & K_1 r_2^2 + d_{n-3} & -d_{n-3} & & \\
 & & & & & -d_{n-3} & c_2 r_3^2 + d_{n-3} & -c_2 r_3 r_4 & \\
 & & & & & & -c_2 r_3 r_4 & c_2 r_4^2 + d_{n-1} & -d_{n-1} \\
 & & & & & & & -d_{n-1} & d_{n-1}
\end{bmatrix} \tag{4}$$

$$K=\begin{bmatrix} k_1 & -k_1 & & & & & & & \\ -k_1 & k_1+k_2 & -k_2 & & & & & & \\ & -k_2 & k_2+k_3 & \ddots & & & & & \\ & & & \ddots & & & & & \\ & & & \ddots & K_1r_1^2+k_{n-5} & -K_1r_1r_2 & & & \\ & & & & -K_1r_1r_2 & K_1r_2^2+k_{n-3} & -k_{n-3} & & \\ & & & & & -k_{n-3} & K_2r_3^2+k_{n-3} & -K_2r_3r_4 & \\ & & & & & & -K_2r_3r_4 & K_2r_4^2+k_{n-1} & -k_{n-1} \\ & & & & & & & -k_{n-1} & k_{n-1} \end{bmatrix} \tag{5}$$

$$P=\begin{bmatrix} T_{in} & 0 & 0 & \cdots & F_1(t)r_1 & -F_1(t)r_2 & F_2(t)r_3 & -F_2(t)r_4 & -T_{out} \end{bmatrix}^{\mathrm{T}} \tag{6}$$

The parameter d signifies the torsional damping of the shaft, while c denotes the meshing damping between gears. The term r represents the pitch circle radius of the gears, and k refers to the torsional stiffness of the shaft. The variable K is indicative of the meshing stiffness between gears. The input and output torques of the system are designated as T_{in} and T_{out}, respectively. The function $F(t)$ accounts for the error excitation between gears.

2.2. Dynamic Modeling of Planetary Wheel Systems

Planetary gear transmission systems, integral to helicopter main reducers, significantly impact the reliability and service life of helicopters due to their vibration and noise. Developing a translational-torsional model focused on a single-stage planetary gear assembly is crucial for assessing these effects. As depicted in Figure 2, this model is essential for analyzing the dynamic behavior within the helicopter's main reducer. The structural parameters of the planetary gears are presented in Table 1.

Compared to pure torsional models, the translational-torsional model incorporates additional nonlinear factors and degrees of freedom, resulting in greater complexity in dynamic modeling and solution processes. To facilitate this, the following three coordinate systems are defined:

1) Global coordinate system (OXY)**:** A fixed coordinate system with its origin at the center of the sun gear. This system does not rotate with the planet carrier.

2) Rotating coordinate system (Oxy)**:** A co-moving system that rotates at a constant angular velocity ω_c, with the planet carrier, with its origin fixed at the center of the carrier.

3) Local coordinate systems ($O_nx_ny_n$ (n = 1, 2, 3))**:** Coordinate systems with their origins at the centers of the planet gears. These systems also rotate at ω_c with the planet carrier, and their axes are aligned with the translational axes of the Oxy system.

The subscripts s, c, r, and denote sun gear, the planet carrier, and ring gear, respectively. Each component has two translational degrees of freedom and one rotational degree of freedom, resulting in a total of 18 degrees of freedom for the model.

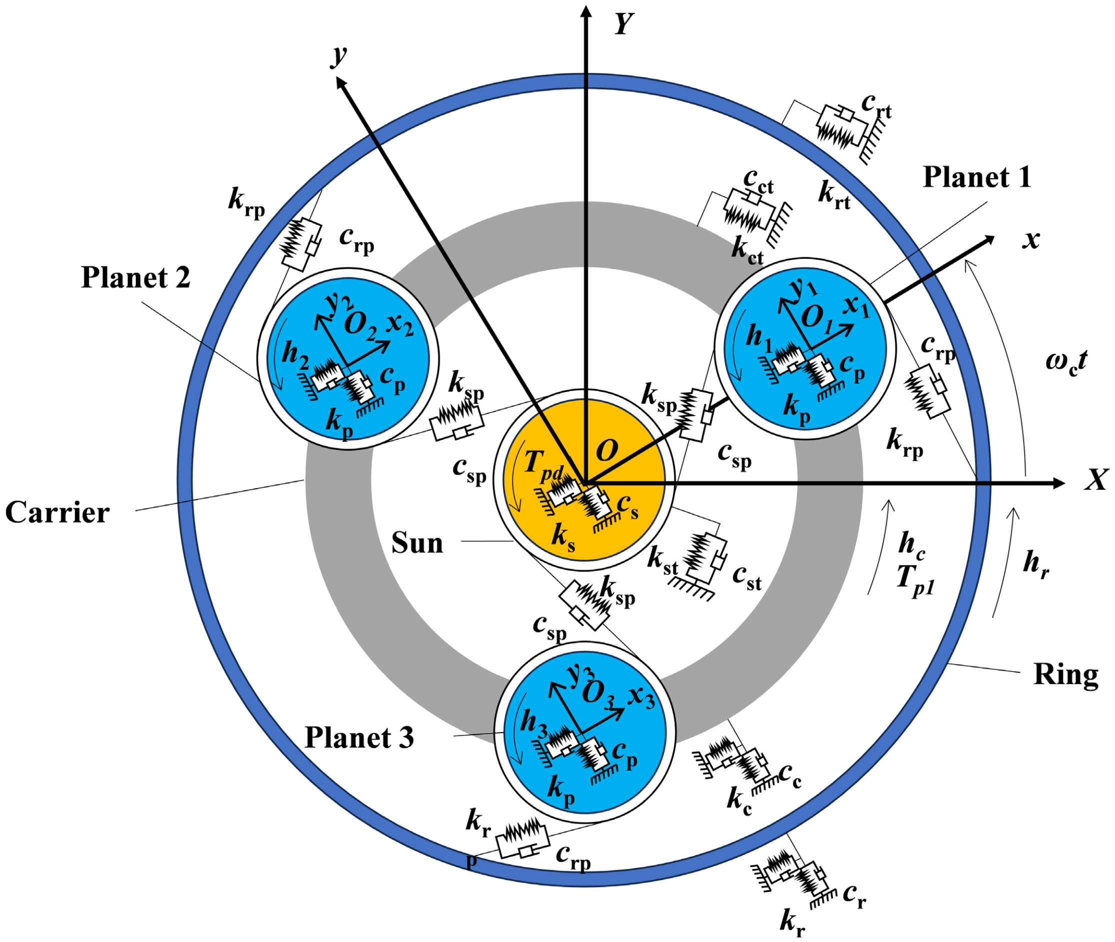

Figure 2. Planetary wheel translational torsion model in helicopter main reducer.

Table 1. Planetary wheel system structure parameters.

	Number of teeth	Modulus	Pressure Angle (˚)	Tooth Width (mm)
Sun Gear	35	4.1	23	70
Planetary	43	4.1	23	68
Ring Gear	125	3.9	15	68

Using Newton's second law, the translational-torsional dynamic model with 18 degrees of freedom, incorporating external loads, is established. The dynamic differential equations for the sun gear, planet carrier, ring gear, and planet gears are derived accordingly:

$$\begin{cases} m_s\left(\ddot{x}_s - 2\omega_c \dot{y}_s - \omega_c^2 x_s\right) - \sum_{n=1}^{3} F_{rpn} \sin\varphi_{rpn} + c_s \dot{x}_s + k_s x_s = 0 \\ m_r\left(\ddot{y}_s + 2\omega_c \dot{x}_s - \omega_c^2 y_s\right) + \sum_{n=1}^{3} F_{rpn} \cos\varphi_{rpn} + c_s \dot{y}_s + k_s y_s = 0 \\ \left(I_s / r_s^2\right)\ddot{h}_s + \sum_{n=1}^{3} F_{rpn} + c_{st}\dot{h}_s / r_s^2 + k_{st} h_s / r_s^2 = T_{pd} / r_s \end{cases} \tag{7}$$

$$\begin{cases} m_c\left(\ddot{x}_c-2\omega_c\dot{y}_c-\omega_c^2x_c\right)+\sum_{n=1}^{3}c_p\dot{\delta}_{cnx}+\sum_{n=1}^{3}k_p\delta_{cnx}+c_c\dot{x}_c+k_cx_c=0 \\ m_c\left(\ddot{y}_c+2\omega_c\dot{x}_c-\omega_c^2y_c\right)+\sum_{n=1}^{3}c_p\dot{\delta}_{cny}+\sum_{n=1}^{3}k_p\delta_{cny}+c_c\dot{y}_c+k_cy_c=0 \\ \left(I_c/r_c^2\right)\ddot{h}_c+\sum_{n=1}^{3}c_p\dot{\delta}_{cnh}+\sum_{n=1}^{3}k_p\delta_{cnh}+c_{ct}\dot{h}_c/r_c^2+k_{ct}h_c/r_c^2=-T_{pl}/r_c \end{cases} \tag{8}$$

$$\begin{cases} m_r\left(\ddot{x}_r-2\omega_c\dot{y}_r-\omega_c^2x_r\right)-\sum_{n=1}^{3}F_{rpn}\sin\varphi_{rpn}+c_r\dot{x}_r+k_rx_r=0 \\ m_r\left(\ddot{y}_r+2\omega_c\dot{x}_r-\omega_c^2y_r\right)+\sum_{n=1}^{3}F_{rpn}\cos\varphi_{rpn}+c_r\dot{y}_r+k_ry_r=0 \\ \left(I_r/r_r^2\right)\ddot{h}_r+\sum_{n=1}^{3}F_{rpn}+c_{rt}\dot{h}_r/r_r^2+k_{rt}h_r/r_r^2=0 \end{cases} \tag{9}$$

$$\begin{cases} m_{pn}\left(\ddot{x}_{pn}-2\omega_c\dot{y}_{pn}-\omega_c^2x_{pn}\right)+F_{spn}\sin\varphi_{spn}+F_{rpn}\sin\varphi_{rpn}-c_{pn}\dot{\delta}_{cnx}-k_{pn}\delta_{cnx}=0 \\ m_{pn}\left(\ddot{y}_{pn}+2\omega_c\dot{x}_{pn}-\omega_c^2y_{pn}\right)-F_{spn}\cos\varphi_{spn}-F_{rpn}\sin\varphi_{rpn}-c_{pn}\dot{\delta}_{cny}-k_{pn}\delta_{cny}=0 \\ \left(I_{pn}/r_{pn}^2\right)\ddot{h}_{pn}+F_{spn}-F_{rpn}=0. \end{cases} \tag{10}$$

In the equations, F_{spn} and F_{rpn} represent the meshing forces between the sun gear and planet gears, and between the ring gear and planet gears, respectively, $F_j=k_j\delta_j+c_j\dot{\delta}_j$ ($j = spn, rpn, n = 1, 2, 3$). The comprehensive transmission error is assumed to vary sinusoidally, expressed as $e_j(t)=E_j\sin\left(2\pi f_m t+\varphi_j\right)$, where E_j *is the error amplitude* and φ_j is the initial meshing phase. By incorporating the influence of gear pair transmission errors, the differential equations are rewritten in matrix form:

$$M\ddot{Q}+\left(C_b+C_m+2\omega_cG\right)\dot{Q}+\left(K_b+K_m-\omega_c^2K_\Omega\right)Q=T_p+E \tag{11}$$

where:

- M is the system mass matrix.
- K_b and C_b are the stiffness and damping matrices for bearing supports.
- K_m and C_m are the stiffness and damping matrices for gear meshing.
- G and K_Ω represent the gyroscopic and centrifugal force matrices.
- Q is the generalized coordinate matrix, composed of displacements in the transverse (x, y) and circumferential (u) directions for all components.
- T_p and E are the torque and error matrices, respectively.

3. Dynamic Characteristic Analysis

After establishing the dynamic model for the helicopter's complete transmission chain, this section focuses on analyzing the vibration response characteristics of the planetary gear system in the main gearbox under several typical flight conditions. The data in this study are dimensionless, and the analysis is descriptive, emphasizing trends.

The vibration response of the planetary gear system on the main gearbox casing is analyzed under four distinct flight conditions: Hovering, Level Flight, Pull Up, and Spiral Turn. The overall vibration response for these conditions is shown in

Figure 3, while Figures 4-7 detail the responses for each flight scenario.

When the input rotational speed causes the gear meshing frequency to coincide with the natural frequency of the gears, resonance occurs, resulting in peak vibration amplitudes. From the response results in Figures 4-7, noticeable peaks are observed near frequencies of 0.057 kHz, 0.093 kHz, and 0.11 kHz under all flight conditions. Additionally, during Hovering, a peak response is also evident at around 0.026 kHz, indicating resonant motion at these frequencies.

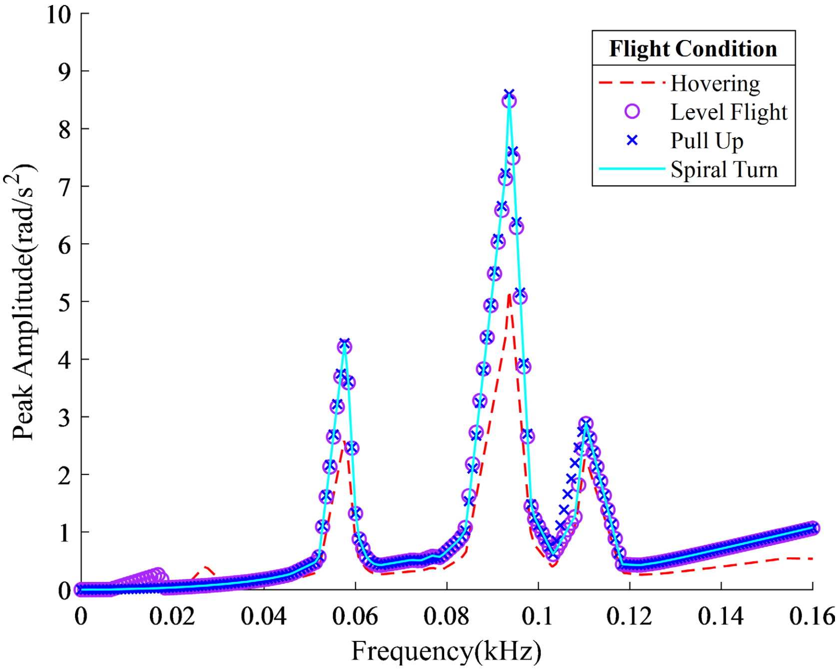

Figure 3. Comparison of vibration response under different flight conditions.

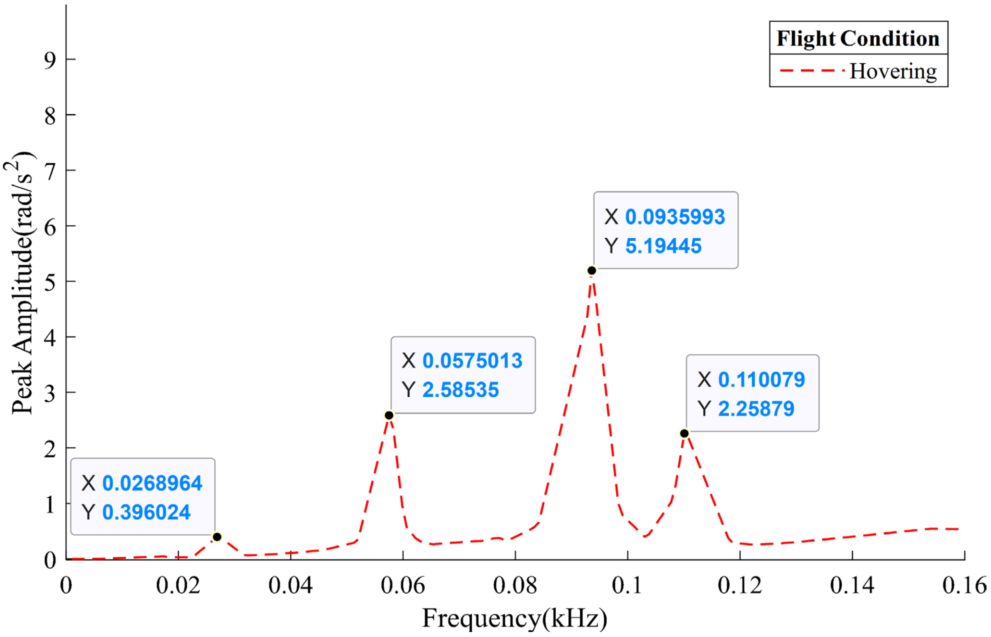

Figure 4. Vibration response under Hovering condition.

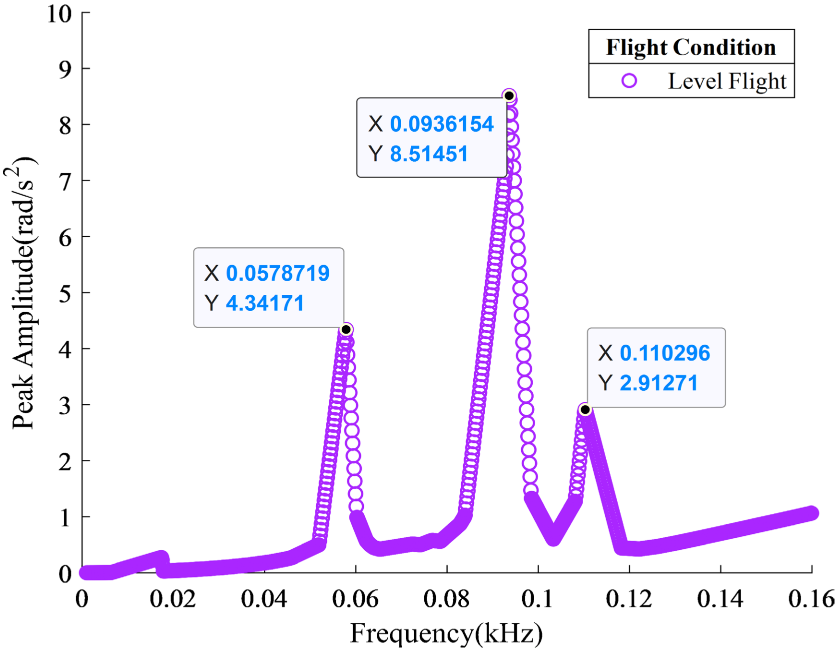

Figure 5. Vibration response under Level Flight condition.

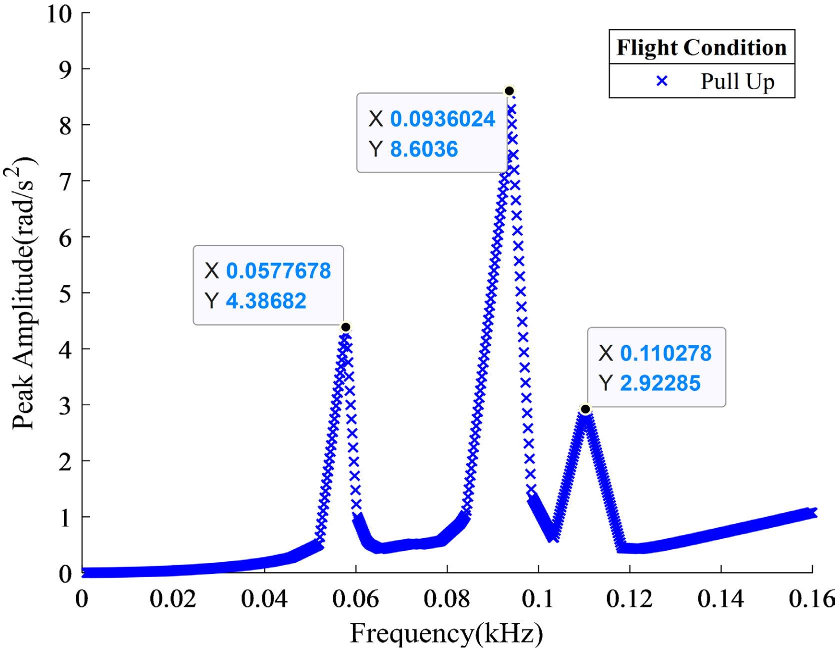

Figure 6. Vibration response under Pull Up condition.

A comparison of the vibration response curves under different flight conditions reveals that the closer the frequency is to the resonance points, the greater the amplitude of the response, reaching a maximum at the resonance frequency. While the trends of the response curves are consistent across all four flight conditions, the amplitude of the resonance response varies. Specifically:

- **Hovering:** Resonance amplitudes at 0.057 kHz, 0.093 kHz, and 0.11 kHz are 2.585 rad/s^2, 5.194 rad/s^2, and 2.259 rad/s^2, respectively.

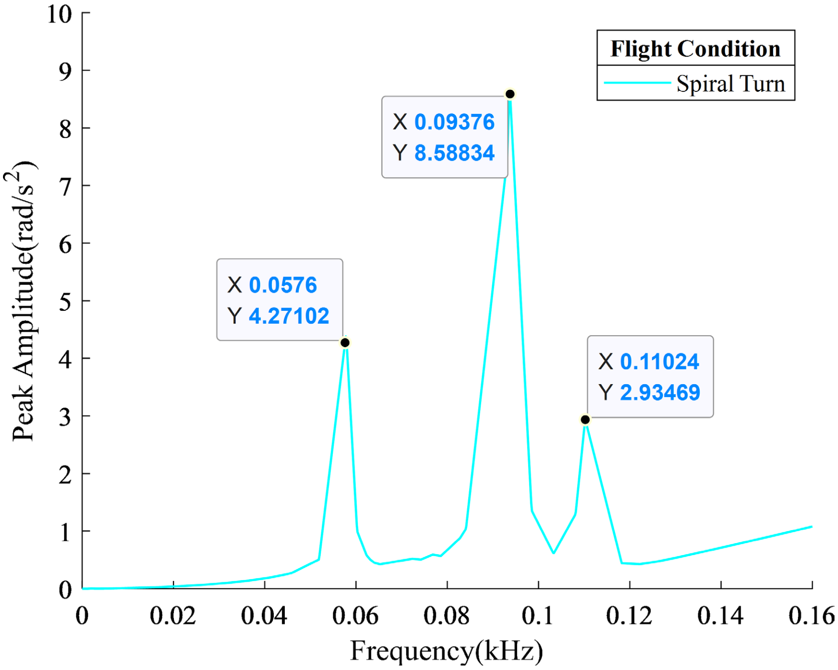

Figure 7. Vibration response under Spiral Turn condition.

- **Level Flight:** Resonance amplitudes at these frequencies are 4.342 rad/s^2, 8.515 rad/s^2, and 2.913 rad/s^2, respectively.
- **Pull Up:** Resonance amplitudes are 4.387 rad/s^2, 8.604 rad/s^2, and 2.923 rad/s^2, respectively.
- **Spiral Turn:** Resonance amplitudes are 4.271 rad/s^2, 8.588 rad/s^2, and 2.934 rad/s^2, respectively.

The resonance amplitudes for Level Flight, Pull Up, and Spiral Turn are similar, while Hovering exhibits significantly lower amplitudes at 0.057 kHz and 0.093 kHz compared to the other flight conditions.

In summary, the resonance frequencies are nearly identical across the different flight conditions, suggesting that these frequencies are intrinsic to the planetary gear system's fundamental parameters. However, the amplitude of the resonance response varies, with Hovering exhibiting relatively lower values, while Level Flight, Pull Up, and Spiral Turn conditions display similar, generally higher amplitudes.

4. Conclusion

A dynamic model of the helicopter transmission system was developed using the lumped mass method, and the dynamic characteristics of the planetary gear system under different flight attitudes were analyzed. The results indicate that: the resonance frequencies of the planetary gear system (0.057 kHz, 0.093 kHz, and 0.11 kHz) remain constant under different flight conditions, suggesting that these frequencies are determined by the inherent structural and dynamic characteristics of the planetary gear system and the vibration amplitudes at resonance points vary across flight conditions. Hovering shows lower resonance amplitudes compared to Level Flight, Pull Up, and Spiral Turn at 0.057 kHz and 0.093 kHz, indicating that operating conditions influence the vibration response. The resonance frequencies and corresponding amplitudes provide critical insights for design and operational safety. Avoiding operating conditions that coincide with resonance frequencies can reduce excessive vibration, enhance performance, and extend the service life of the transmission system.

Conflicts of Interest

The authors declare no conflicts of interest regarding the publication of this paper.

References

[1] She, Y.X., Kang, L.X. and Tang, P. (2021) Research on the Current Status and Development of Helicopter Transmission Systems. *Aviation Science and Technology*, **1**, 78-82. https://doi.org/10.19452/j.issn1007-5453.2021.01.013

[2] Bao, H.Y., Li, F.B., Lu, F.X., Jin, G.H., Zhu, R.P. and Zou, X.Z. (2019) Dynamic Characteristics Analysis of a Variable-Speed Helicopter Transmission System. *Journal of Central South University* (*Natural Science Edition*), **10**, 2403-2416.

[3] Wei, Y. and Chen, R.L. (2024) Dynamic Modeling and Response Analysis of Helicopter/Engine Coupling Systems. *Journal of Harbin Institute of Technology*, 56, 1-9.

[4] Chen, G.W., Tang, Q., Li, H. and Yang, Z. (2024) Predictive Modeling and Experimental Study of Helicopter Tail Transmission System Responses. *Journal of Aerospace Power*, 1-15. https://doi.org/10.13224/j.cnki.jasp.20240364

[5] Ni, D., Zhong, T.J., Wei, J., Cao, M.F. and Peng, B. (2022) Calculation and Optimization of Torsional Vibration in the Rotor Shaft of a Helicopter Transmission System. *Mechanical Transmission*, **1**, 80-86. https://doi.org/10.16578/j.issn.1004.2539.2022.01.010

[6] Li, H., Yang, X.G., Luo, Z.Y. and Bao, H.Y. (2022) Design and Analysis of a Variable-Speed Transmission System for Helicopters. *Mechanical Engineer*, **2**, 93-95, 98.

[7] Long, L., Li, J., Zhao, Y.M. and Wang, D. (2021) Coupled Vibration Characteristics of the Power Transmission Shaft-Casing System. *Science Technology and Engineering*, **21**, 14422-14427.

[8] Zeng, L. (2022) Research on Design Methods for Helicopter Transmission System Configurations. Master's Thesis, Chongqing University.

[9] Luo, L.L. (2021) Research on the Design Method of the Main Reducer Configuration of the Helicopter Transmission System. *Electromechanical Engineering Technology*, **50**, 206-208.

[10] Zhu, H., Chen, W., Zhu, R., Zhang, L., Fu, B. and Lu, X. (2021) Modeling and Dynamic Analysis of Spiral Bevel Gear Coupled System of Intermediate and Tail Gearboxes in a Helicopter. *Proceedings of the Institution of Mechanical Engineers*, *Part C: Journal of Mechanical Engineering Science*, **235**, 5975-5993. https://doi.org/10.1177/0954406221992798